

Published in final edited form as:

Nat Cell Biol. 2011 February ; 13(2): 159–166. doi:10.1038/ncb2156.

Spatially restricted activation of RhoA at epithelial junctions by p114RhoGEF drives junction formation and morphogenesis

Stephen J. Terry¹, Ceniz Zihni¹, Ahmed Elbediwy¹, Elisa Vitiello¹, Isabelle V. Leefa Chong San¹, Maria S. Balda^{1,*}, and Karl Matter^{1,*}

¹Department of Cell Biology, UCL Institute of Ophthalmology, University College London, Bath Street, London EC1V 9EL, UK

Abstract

Signalling by the GTPase RhoA, a key regulator of epithelial cell behaviour, can stimulate opposing processes: RhoA can promote junction formation and apical constriction, as well as reduced adhesion and cell spreading^{1, 2}. Molecular mechanisms are thus required that ensure spatially restricted and process-specific RhoA activation. For many fundamental processes, including assembly of the epithelial junctional complex, such mechanisms are still unknown. Here we show that p114RhoGEF is a junction-associated protein that drives RhoA signalling at the junctional complex and regulates tight junction assembly and epithelial morphogenesis. p114RhoGEF is required for RhoA activation at cell-cell junctions, and its depletion stimulates non-junctional Rho signalling and induction of myosin phosphorylation along the basal domain. Depletion of GEF-H1, a RhoA activator inhibited by junctional recruitment³, does not reduce junction-associated RhoA activation. p114RhoGEF associates with a complex containing myosin II, Rock II and the junctional adaptor cingulin, indicating that p114RhoGEF is a component of a junction-associated Rho signalling module that drives spatially restricted activation of RhoA to regulate junction formation and epithelial morphogenesis.

A particular RhoGTPase can be part of signalling mechanisms that stimulate opposing processes and, at a given point in time, may be activated at one subcellular site and inactivated at another. Orchestration of RhoGTPase signalling thus requires mechanisms that regulate activity in space and time^{4, 5}. Activation of GTPases is catalysed by guanine nucleotide exchange factors (GEFs) and inactivation by GTPase activating proteins (GAPs)^{2, 6}. In epithelial cells, the RhoGTPase family member RhoA is activated at cell junctions upon initiation of cell-cell adhesion and, concomitantly, downregulated in other parts of the cells, contributing to reduced cell spreading and stress fibre formation, and inhibition of proliferation⁷⁻¹³. Junctional RhoA activation drives formation of tight and adherens junctions, and is required to maintain junctional integrity, processes that are mediated by the actinomyosin cytoskeleton; however, how RhoA is activated at junctions is not understood. GEF-H1, a GEF for RhoA, localises to tight junctions, the most apical component of the junctional complex; yet, it is not required for junction formation, and junctional recruitment leads to its inactivation and inhibition of the Rho-stimulated

*Corresponding authors: Tel – 44 20 7608 4014, Fax – 44 20 7608 4034, k.matter@ucl.ac.uk/m.balda@ucl.ac.uk.

[†]Contributed equally

AUTHOR CONTRIBUTIONS

SJT performed most of the experiments. All other authors performed particular subsets of experiments. SJT, MSB and KM designed the project and wrote the manuscript.

COMPETING INTERESTS

The authors declare that they have no competing financial interests.

transcription factor ZONAB^{3, 14, 15}. GEF-H1 activation is indeed required for junction dissociation¹⁶.

We identified p114RhoGEF as a regulator of epithelial differentiation and junction assembly using a functional siRNA screen. A p114RhoGEF-specific antibody was found to detect a 114kD protein that disappeared upon transfection of specific siRNAs in the human intestinal epithelial cell line Caco-2 and in immortalised human corneal epithelial (HCE) cells (Fig. 1a). By immunofluorescence, this antibody stained the junctional complex and a cytoplasmic pool (Fig. 1b). Both stainings disappeared upon p114RhoGEF depletion (Fig. 1c). Junctional p114RhoGEF overlapped with occludin, a tight junction protein, but not E-cadherin, an adherens junction component, indicating that p114RhoGEF associates with the apical junctional complex and tight junctions (Fig. 1d,e).

p114RhoGEF is a widely expressed gene and, *in vitro*, functions as a specific activator of RhoA¹⁷⁻¹⁹. Accordingly, depletion of p114RhoGEF resulted in reduced levels of active RhoA in HCE cells without significantly affecting Rac and Cdc42 (Fig. 1f).

We next determined the effect of p114RhoGEF depletion on the junctional complex by staining for tight and adherens junction markers. In the columnar epithelial cell line Caco-2, p114RhoGEF depletion resulted in flatter cells and in a warped appearance of the junctional staining of ZO-1 and, to a lesser degree, β -catenin, as well as reduced perijunctional f-actin and increased formation of stress fibres (Fig. 1g,h). The phenotype of HCE cells was similar but, as these are not columnar, no flattening was observed. Strikingly, ZO-1 staining was disrupted, indicating a defect in tight junction assembly. Comparable phenotypes were observed when cells were stained for other tight junction markers and when p114RhoGEF was depleted with individual siRNAs or a different type of siRNA pool (Fig. S1). p114RhoGEF is thus required for normal junction formation and actin organisation.

We next investigated if Caco-2 cells depleted of p114RhoGEF form functional epithelial barriers by testing the permeability properties of the monolayers (Fig. 2 a - c). We performed calcium switch assays to monitor *de novo* junction formation and measured transepithelial electrical resistance, a measure of barrier integrity²⁰. Depletion of p114RhoGEF strongly attenuated barrier formation and only reached 40% of the values of control cultures (Fig. 2b). Paracellular diffusion of fluorescent 4 and 70 kD dextran was still high in such cultures, indicating that tight junctions remained leaky (Fig. 2c).

Morphological analysis of cells incubated for different times with calcium revealed that p114RhoGEF depletion did not affect initial spreading and initiation of cell-cell contacts as ZO-1 accumulated at forming junctions already after 1 hour and f-actin staining revealed spread cells (Fig. 2d,e,f). However, ZO-1 staining remained discontinuous and warped even after 24 hours. Similar observations were made for other junctional markers (Fig. S2a). Thus, p114RhoGEF is not required for spreading and initiation of adhesion, but for junctional maturation. As expected, GEF-H1 depleted cells spread more slowly as round cells were still detected after 1 hour with calcium but, once junctions started to form, they established morphologically normal junctions (Fig. 2d,e). GEF-H1 depletion did also not affect junction formation in HCE cells (Fig. S2b,c). This is in agreement with previous observations indicating that GEF-H1 is not required for junction formation but cell spreading^{14, 16, 21}.

p114RhoGEF localised to forming junctions already after 30 minutes together with myosin II, a target of Rho signalling during junctional maturation¹³ (Fig. 2g). Myosin II recruitment to cell contacts was attenuated by p114RhoGEF depletion and, instead, showed increased association with stress fibres (Fig. 2g and S2d). GEF-H1 was also not recruited to cell

contacts and may hence contribute to the increase in stress fibres along the base of the cells^{15, 22}.

We next analysed whether p114RhoGEF regulates epithelial morphogenesis using three-dimensional culture systems that allow the formation of polarised cysts with a central lumen²³. p114RhoGEF was depleted by siRNA transfection in Caco-2 cells and expression of shRNAs in MDCK cells (Fig. S2e). Depletion affected both epithelial cell types, resulting in a disorganised appearance of the cysts that often developed multiple lumens and an irregular distribution of ZO-1 (Fig. 3). The apical marker podocalyxin still accumulated in lumens, suggesting p114RhoGEF depletion did not cause a loss of polarity but a disorganised three-dimensional arrangement of the cells.

We next investigated whether p114RhoGEF stimulates Rho signalling at the junctional complex. We used a FRET (Fluorescence Resonance Energy Transfer)-based RhoA biosensor to localise RhoA activation in live cells after depletion of either p114RhoGEF or, as an additional control, GEF-H1²⁴. In control cells, the most intense FRET signal, indicating active RhoA, was observed along cell-cell junctions (Fig. 4a). Depletion of p114RhoGEF led to a redistribution of the FRET signal away from cell junctions and was increased throughout the cells including the basal domain (Fig. 4a,b and S3a). Depletion of GEF-H1 did not affect the junctional FRET signal. Comparable results were obtained with HCE and Caco-2 cells as well as during junction formation, indicating that p114RhoGEF is required for spatially restricted RhoA activation at cell junctions.

One of the main targets of RhoA signalling is phosphorylation of the light chain of myosin II (MLC), leading to myosin activation². Therefore we next investigated the role of p114RhoGEF in MLC phosphorylation. In control cells, myosin staining was found along the junctional complex and, to a lesser extent, along the basal membrane (Fig. 4c,d). Depletion of p114RhoGEF led to a redistribution of myosin from junctions to stress fibres. Phosphorylated MLC was found along cell junctions in control cells and concentrated on stress fibres in the absence of p114RhoGEF, indicating that myosin activation was shifted to the basal domain. GEF-H1 depletion did not affect the distribution of phosphorylated MLC (Fig. 4d). Depletion of p114RhoGEF also inhibited the appearance of phosphorylated MLC during junction assembly, indicating that it is required for myosin activation during junction formation (Fig. S4a). p114RhoGEF depletion did not alter total levels of phosphorylated MLC in Caco-2 cells and only slightly reduced them in HCE cells (Fig. S4b). Phosphorylation of the Rock substrate myosin light chain phosphatase was also unaltered. These observations suggest that p114RhoGEF is required for the spatially restricted activation of RhoA signalling and myosin activation at cell-cell junctions, and that its absence leads to defective junction assembly, cell spreading, increased non-junctional RhoA signalling and myosin activation.

If p114RhoGEF regulates activation of junctional myosin, overexpression should induce junctional actinomyosin contraction and this should require a functional GEF domain. Hence, we substituted a conserved tyrosine residue in the Dbl domain necessary for GEF activity (p114RhoGEFY260A). Analogous mutations were previously shown to inactivate the GEF activities of GEF-H1 and Lbc^{25, 26}. Cells expressing VSV-tagged p114RhoGEF had increased active RhoA levels and increased levels of phosphorylated MLC whereas expression of the mutant had no effect (Fig. 4e and S4c). Morphologically, expression of p114RhoGEF-VSV led to an apically contracted, rounded morphology with increased perijunctional f-actin (Fig. 4f,g). In stably transfected MDCK cells, upregulation of the active p114RhoGEF led to increased phosphorylated MLC at cell junctions (Fig. S4d). Expression of active, but not inactive p114RhoGEF led to Rock activity-dependent rounding and monolayer contraction leading to monolayer gaps (Fig. S4e). Cell compaction was

particularly striking in the normally flat HCE cells, which developed an apically elongated, dome-like appearance with a contracted junctional ring, but was also evident in Caco-2 cells (Fig. 4f,g, h and S5a). These effects required Rho activation as they were not observed when p114RhoGEFY260A-VSV was expressed. Similarly, only active human p114RhoGEF could induce recruitment of junctional markers in depleted MDCK cells, and expression of the inactive exchange factor in HCE cells interfered with the normal junctional distribution of ZO-1 (Fig. S5b,c,d). Overexpression of GEF-H1 did not induce contraction of the perijunctional actinomyosin ring (Fig. 4f). These data indicate that junctional contraction is a p114RhoGEF-specific function and requires a functional GEF domain.

As p114RhoGEF regulates the junctional recruitment of myosin, we next tested whether the two proteins are part of a common complex. p114RhoGEF immunoprecipitates contained myosin IIA and the RhoA effector Rock II (Fig. 5a). Cingulin, a tight junction-associated adaptor known to form a complex with myosin and to regulate RhoA signalling, was also coprecipitating with p114RhoGEF (Fig. 5a)^{3, 27}. Coprecipitation of myosin IIA, cingulin and RockII was not detected when cells were not allowed to form junctions by culturing in low calcium medium. Cingulin can also bind GEF-H1; however, coprecipitation of the two GEFs was not observed (not shown), suggesting that they are part of distinct complexes.

We next used GST fusion proteins of p114RhoGEF to map the domain of p114RhoGEF required for these interactions (Fig 5b). We found that full-length p114RhoGEF pulled down myosin IIA, cingulin and Rock II; however, the efficiency was low possibly because the full length fusion protein was difficult to express. The PH domain alone pulled down myosin and cingulin efficiently. Pull down of Rock II was not efficient, suggesting that Rho activation might be needed for efficient Rock recruitment.

We next asked whether cingulin is required for recruitment of p114RhoGEF to tight junctions. Depletion of cingulin indeed inhibited junctional recruitment of p114RhoGEF (Fig. 5c,d,e). In HCE cells, cingulin was required for tight junction formation: depletion led to a loss of junctional staining not only of p114RhoGEF, but also of ZO-1, occludin and GEF-H1, but not of components of adherens junctions (Fig. 5 and S6a,b,c). Cingulin and p114RhoGEF also colocalised by confocal microscopy, and overexpression of cingulin led to a redistribution of p114RhoGEF and myosin (Fig. S6d,e). Cingulin depletion also attenuated p114RhoGEF and myosin IIA recruitment, and MLC phosphorylation at forming junctions (Fig. S6f). Similarly, cingulin was required for myosin recruitment and MLC phosphorylation in HCE cells, and for normal Rho activation at cell junctions in Caco-2 and HCE cells (Fig. 5f and S3). Cingulin is thus important for the cellular distribution of p114RhoGEF and for activation of RhoA signalling at cell junctions.

Our study shows that p114RhoGEF regulates spatially restricted activation of RhoA at epithelial junctions, driving junction assembly and junctional actinomyosin activation. RhoA signalling is well-known to be a crucial regulator of junction assembly and function¹; however, the GEF that activates RhoA at cell junctions had thus far not been known. p114RhoGEF forms a functional signalling module containing Rock II and myosin, two proteins that are known to regulate junction dynamics^{16, 28}. Junctional recruitment requires cingulin, an adaptor protein that is known to impact on RhoA signalling^{3, 29}.

p114RhoGEF regulates spatially restricted RhoA activation at cell-cell contacts in different types of epithelial cells. In agreement with previous results, depletion of GEF-H1, which is not required for junction formation and is inactive at junctions, did not affect junctional Rho signalling^{3, 14}. Hence, p114RhoGEF and GEF-H1 represent two opposing pathways of RhoA regulation at cell junctions: the former is recruited to the forming junctional complex and promotes junctional maturation and contraction of the actinomyosin belt; the latter is

recruited and turned off, contributing to inhibition of confluence-induced RhoA signalling and cell proliferation.

Depletion of p114RhoGEF did not only inhibit RhoA activation at junctions, but led to increased non-junctional Rho activation and increased MLC phosphorylation along the basal domain. Paradoxically as this may seem, it supports the specificity of p114RhoGEF for junctional Rho signalling and its importance for junction formation. RhoA activity is downregulated in response to cell confluence; hence, interfering with junction formation stimulates RhoA signalling in the rest of the cell³⁰. As junctions do not form normally in p114RhoGEF depleted cells, GEF-H1 is also not recruited normally and, hence, is likely to contribute to overall RhoA activation in such cells. GEF-H1 indeed induces stress fibres in response to stimuli such as TNF α ^{15, 22}. However, there are other mechanisms that contribute to inhibition of RhoA signalling at cell confluence, such as regulation of p190RhoGAP³¹ or, possibly, the junction-associated GAP myosin-IXb³², and depletion of GEF-H1 in addition to p114RhoGEF was not sufficient to block stress fibre formation (not shown).

The junction-associated actinomyosin cytoskeleton is crucial for the regulation of junction dynamics and function, and also drives apical constriction and tissue remodeling¹. p114RhoGEF thus associates with and activates a Rho signalling module that is central to epithelial junction formation and morphogenesis. This is supported by our data that shows p114RhoGEF regulated junction assembly and epithelial morphogenesis in three-dimensional culture systems. Overexpression of p114RhoGEF induced actinomyosin contraction, suggesting that this Rho GEF may also be important for developmental processes requiring apical constriction.

Our data thus show that p114RhoGEF represents a RhoA regulator central to epithelial barrier formation and morphogenesis that forms a junction-associated signalling module. Given the physiological roles of junctional RhoA signalling, it will be important to determine how p114RhoGEF becomes stimulated during physiological and developmental processes to drive spatially restricted Rho signalling at cell junctions.

Supplementary Material

Refer to Web version on PubMed Central for supplementary material.

Acknowledgments

SJT is supported by a Fight for Sight Studentship. This research was supported by Fight for Sight and the Wellcome Trust.

Methods

DNA constructs, RNA interference

A construct containing the human p114RhoGEF cDNA sequence was kindly provided by T. Voino-Yasenetskaya (University of Illinois at Chicago, Chicago, Illinois, USA)¹⁹. The cDNA was used to generate VSV-tagged constructs that were cloned into pCDNA4/TO (Invitrogen). The point mutation Y260-A was introduced with the Quickchange mutagenesis kit (Stratagene) and the primers 5'-CGCATAACCAAAGCCCCAGTGCTGGTGG-3' and 5'-CACCAGCACTGGGGCTTTGGTTATGCG-3'. For p114RhoGEF GST fusion proteins the sequences encoding the indicated domains were cloned into pGEX-4T-3 (GE Lifesciences) to generate GST-N-terminally-tagged fusion proteins. The tetracycline repressor was expressed with pcDNA6/TR (Invitrogen). The GEF-H1-VSV and myc-

cingulin cDNAs were as described³. For RNAi experiments cells were transfected with individual or pools of siGenome or On-Target plus siRNAs for p114RhoGEF (ARHGEF18), Cingulin (CGNL1) and GEF-H1 (ARHGEF2) as well as non-targeting control siRNAs (Thermo Scientific, Dharmacon). All experiments shown using GEF-H1 siRNAs were performed with the siGenome version as they were more effective than On-Target plus siRNAs. The sequences were 5'-GGACAAGCCUUCAGUGGUA-3', 5'-CAACAUUGCUGGACAUUUC-3', 5'-GAAUUAAGAUGGAGUUGCA-3' and 5'-GUGCGGAGCAGAUGUGUAA-3'. Sequences for individual p114RhoGEF siGenome siRNAs were 5'-UCAGGCGCUUGAAAGAU-3' and 5'-GGACGCAACUCGGACCAAU-3'. For MDCK cells, the sequences 5'-AAGACCACGTCGGGACGCTTG-3' and 5'-AACTACGTCATCCAGAAAATC-3' were targeted using either siRNAs or by expressing shRNAs using a plasmid with a tetracycline-regulated mouse U6 promoter³. For cingulin, the sequences were 5'-GGACCAGGGUGAAGAUUUA-3' and 5'-GGACACAGGAGGAGCUUAA-3'. For siRNA transfections, Interferin transfection reagent (Polyplus-transfection Inc.) was used according to the manufacturer's instructions using a total final siRNA concentration of 40 nM. Caco-2 cells were transfected one day after plating, and HCE and MDCK cells 1 hour after seeding. Samples were collected and processed 3 – 4 days after transfection or, for the morphogenesis experiments, after 5 days. For DNA transfections 0.3 µg/ml plasmid DNA and JetPEI transfection reagent (Polyplus-transfection Inc.) were used according to the manufacturer's instructions. Samples were collected and processed after 24 hours.

Antibodies

Antibodies used were as follows: goat anti-p114 RhoGEF (ARHGEF18) (immunoblotting, 1/1000; immunofluorescence, 1:200), Everest Biotech; mouse anti-occludin (1/1000), mouse anti-ZO-1 (immunofluorescence, 1:1000) and rabbit anti-cingulin (immunoblotting, 1/5000; immunofluorescence, 1:1000), Invitrogen; goat anti-β-catenin (immunofluorescence, 1:100) and rabbit anti-cingulin (1:1000), Santa Cruz Biotech; guinea pig anti-occludin (immunofluorescence, 1:200), Hycult Biotech; rabbit anti-myosin IIA (1:1000), anti-β-catenin (1:1000) and α-catenin (1:1000), Sigma-Aldrich; mouse anti-E-cadherin (immunoblotting, 1/1000; immunofluorescence, 1:500), anti-p120catenin (immunoblotting, 1/1000; immunofluorescence, 1:500), anti-cofilin (immunoblotting, 1/500), anti-Rock II (immunoblotting, 1/1000; immunofluorescence, 1:200), BD Biosciences; rabbit anti-MLC (immunoblotting, 1/500; immunofluorescence, 1:200), anti-ppMLC (T18,S19) (immunoblotting, 1/500; immunofluorescence, 1:200) and phospholyated Cofilin (immunoblotting, 1/500), Cell signalling Technologies; total (immunoblotting, 1/5000) and phosphorylated (T696) (immunoblotting, 1/1000) myosin light chain phosphatase MYPT1, Millipore. Antibodies against ZO-1 (rabbit: immunoblotting, 1/1000; immunofluorescence, 1:500; note, this antibody crossreacts with a nuclear antigen in human cells.), α-tubulin (mouse: immunoblotting, 1/400), GEF-H1 (mouse: immunofluorescence, 1/10; rabbit: immunoblotting, 1/500), VSV (mouse: immunofluorescence, 1/10; immunoblotting, 1/20) and myc (mouse: immunofluorescence, 1/100) epitopes were described previously¹⁴.

Cell culture and cell lines

Human adenocarcinoma colon cells (Caco-2)³³ and human corneal epithelial cells (HCE), transformed with SV-40 T antigen, (Gift from M.S. Chang, Vanderbilt University, Nashville, Tennessee, USA)³⁴ and Madin-Darby Canine Kidney cells (MDCK) were cultured in DMEM containing 10% heat inactivated FBS (20% FBS for Caco-2) with 100 µg/ml streptomycin and 100 µg/ml penicillin (PAA cell culture) at 37°C in a 5% CO₂ atmosphere. Stable MDCK cell lines were generated as described³. The three dimensional

cultures of MDCK cells were generated as previously³⁵, and, for Caco-2 cells, a recently described method was used³⁶.

Calcium switch and permeability assays

Caco-2 cells were cultured in six well plates for the siRNA transfections and, after 24 hours, were trypsinised and replated in low calcium medium containing dialysed FBS³⁷. After another 24 hours, normal medium was added to induce junction formation. Samples were fixed at various time points for immunostaining. Transepithelial electrical resistance (TER) measurements were taken using an AC square wave current of $\pm 20 \mu\text{A}$ at 12.5 Hz with a silver electrode and measuring the voltage deflection elicited with a silver/silver-chloride electrode using an EVOM (World Precision Instruments, Sarasota, FL) as previously described³⁸. Paracellular permeability was determined using 4 kD FITC-conjugated Dextran and 70 kD Rhodamine B-conjugated dextran over a time of 3 hours³⁸. Fluorescence was then determined with a FLUOstar OPTIMA microplate reader (BMGLabTech, Offenburg, Germany).

Immunostaining and microscopy

Cells were fixed in methanol or 3% PFA as previously described¹⁴ and stained with the appropriate fluorescent secondary antibodies conjugated to either FITC, Cy3, Cy5 or AMCA (1:600 dilutions; Jackson ImmunoResearch Inc.) or incubated with FITC or TRITC conjugated Phalloidin (Sigma) or DNA stain Hoechst 33258 (Invitrogen). Slides were observed under a Leica DMIRB fluorescent microscope, and Zeiss LSM 510 and 700 confocal laser scanning microscopes using 63x immersion oil lenses. Images were acquired using simple PCI and LSM510 and ZEN operating softwares, respectively. Image were adjusted for brightness and contrast with Adobe Photoshop. For FRET experiments, siRNA transfected cells were plated into ibid multi-well chamber slides and then transfected with pRaichu-RhoA (kindly provided by M. Matsuda, Osaka University, Japan)²⁴. The FRET analysis was performed at 37°C with a Leica SP2 microscope using the manufacturer's software measuring donor recovery after acceptor bleaching (YFP was bleached to 30%). FRET efficiency maps were then produced with the Leica software. For quantification, CFP images were subtracted and then quantified with ImageJ. For each image, all cell-cell contacts were quantified and as many internal areas; averages of all cell-cell contacts and all internal areas then gave one value each per image, and these values were used for the final statistical analysis. Normalisations were performed by dividing values obtained for specific fields by the values obtained for the entire field imaged.

Immunoblotting, immunoprecipitations, GST pull downs, RhoGTPase activation assays

Whole cell lysates were collected by washing twice with PBS before adding SDS-PAGE sample buffer and heating at 70°C for 10 minutes before homogenising with a 23G needle. Samples were processed using standard western blotting techniques. Protein-bound antibodies were detected with horseradish peroxidase conjugated secondary antibodies using enhanced chemiluminescence detection system (ECL, Amersham, Corp. Arlington Heights, IL), or IRDye-680- and IRDye-800CW-conjugated secondary antibodies and an Odyssey detector (LI-COR). For immunoprecipitations, Caco2 cells were extracted at 4°C with 10 mM Hepes (pH 7.4), containing 150 mM NaCl, 1% Triton X-100, 0.5% sodium deoxycholate, 0.2% SDS and a cocktail of protease and phosphatase inhibitors as previously described¹⁴. Extracts were pre-adsorbed with inactive sepharose beads for 15 minutes prior to incubation with antibodies conjugated to Protein G sepharose beads for 2 hours at 4°C. Samples were washed twice with 0.5% Triton X-100 in PBS and once with PBS before

adding SDS-PAGE sample buffer. For GST pull-down experiments with p114RhoGEF fusion proteins, cells were extracted with the same buffer at 4°C and preadsorbed with inactive beads as above for immunoprecipitations. Extracts were incubated with glutathione-agarose beads coated with 15 µg of fusion proteins and incubated for 2 hours at 4°C before washing as described for immunoprecipitations. For RhoGTPase activation assays, cells were transfected with the appropriate siRNAs in 12-well plates and, after 72 hours, protein was harvested and analysed for levels of active RhoA, Cdc42 and Rac1 using the respective G-LISA assay kits from Cytoskeleton Inc. Protein concentrations were equilibrated before incubation with the coated 96-well plates and HRP conjugated secondary antibodies were used for detection. Samples of cell extracts were immunoblotted for the GTPases to exclude altered expression levels.

Statistical analysis

Averages and standard deviations were calculated and provided in the graphs. Respective n values are provided in the figure legends. The indicated p values were obtained with two-tailed Student's t-test.

REFERENCES

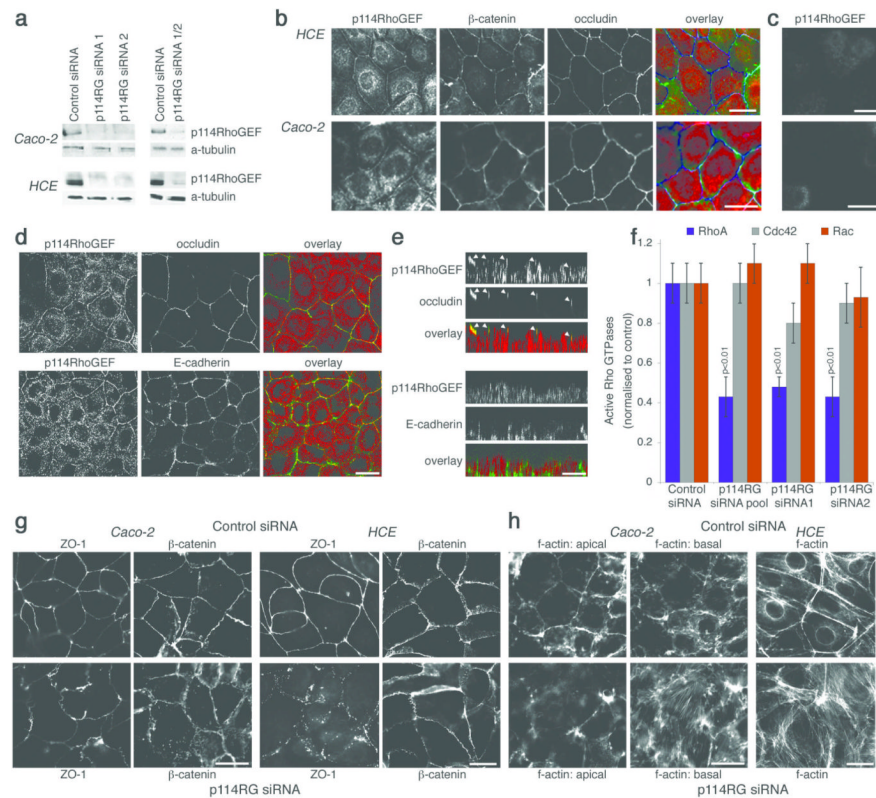
1. Terry S, Nie M, Matter K, Balda MS. Rho signaling and tight junction functions. *Physiology* (Bethesda). 2010; 25:16–26. [PubMed: 20134025]
2. Etienne-Manneville S, Hall A. Rho GTPases in cell biology. *Nature*. 2002; 420:629–635. [PubMed: 12478284]
3. Aijaz S, D'Atri F, Citi S, Balda MS, Matter K. Binding of GEF-H1 to the tight junction-associated adaptor cingulin results in inhibition of Rho signaling and G1/S phase transition. *Dev Cell*. 2005; 8:777–786. [PubMed: 15866167]
4. Pertz O. Spatio-temporal Rho GTPase signaling - where are we now? *J Cell Sci*. 2010; 123:1841–1850. [PubMed: 20484664]
5. Heasman SJ, Ridley AJ. Mammalian Rho GTPases: new insights into their functions from in vivo studies. *Nat Rev Mol Cell Biol*. 2008; 9:690–701. [PubMed: 18719708]
6. Rossman KL, Der CJ, Sondek J. GEF means go: turning on RHO GTPases with guanine nucleotide-exchange factors. *Nat Rev Mol Cell Biol*. 2005; 6:167–180. [PubMed: 15688002]
7. Nusrat A, et al. Rho protein regulates tight junctions and perijunctional actin organization in polarized epithelia. *Proc. Natl. Acad. Sci. U S A*. 1995; 92:10629–10633. [PubMed: 7479854]
8. Braga VM, Machesky LM, Hall A, Hotchin NA. The small GTPases Rho and Rac are required for the establishment of cadherin-dependent cell-cell contacts. *J. Cell Biol*. 1997; 137:1421–1431. [PubMed: 9182672]
9. Noren NK, Niessen CM, Gumbiner BM, Burrige K. Cadherin engagement regulates Rho family GTPases. *J. Biol. Chem*. 2001; 276:33305–33308. [PubMed: 11457821]
10. Zondag GC, et al. Oncogenic Ras downregulates Rac activity, which leads to increased Rho activity and epithelial-mesenchymal transition. *J. Cell Biol*. 2000; 149:775–782. [PubMed: 10811819]
11. Coleman ML, Marshall CJ, Olson MF. RAS and RHO GTPases in G1-phase cell-cycle regulation. *Nat Rev Mol Cell Biol*. 2004; 5:355–366. [PubMed: 15122349]
12. Ozdamar B, et al. Regulation of the polarity protein Par6 by TGFbeta receptors controls epithelial cell plasticity. *Science*. 2005; 307:1603–1609. [PubMed: 15761148]
13. Yamada S, Nelson WJ. Localized zones of Rho and Rac activities drive initiation and expansion of epithelial cell-cell adhesion. *J Cell Biol*. 2007; 178:517–527. [PubMed: 17646397]
14. Benais-Pont G, et al. Identification of a tight junction-associated guanine nucleotide exchange factor that activates Rho and regulates paracellular permeability. *J Cell Biol*. 2003; 160:729–740. [PubMed: 12604587]

15. Nie M, Aijaz S, Leefa Chong San IV, Balda MS, Matter K. The Y-box factor ZONAB/DbpA associates with GEF-H1/Lfc and mediates Rho-stimulated transcription. *EMBO Rep.* 2009; 10:1125–1131. [PubMed: 19730435]
16. Samarín SN, Ivanov AI, Flatau G, Parkos CA, Nusrat A. Rho/Rho-associated kinase-II signaling mediates disassembly of epithelial apical junctions. *Mol Biol Cell.* 2007; 18:3429–3439. [PubMed: 17596509]
17. Blomquist A, et al. Identification and characterization of a novel Rho-specific guanine nucleotide exchange factor. *Biochem J.* 2000; 352(Pt 2):319–325. [PubMed: 11085924]
18. Nagata K, Inagaki M. Cytoskeletal modification of Rho guanine nucleotide exchange factor activity: identification of a Rho guanine nucleotide exchange factor as a binding partner for Sept9b, a mammalian septin. *Oncogene.* 2005; 24:65–76. [PubMed: 15558029]
19. Niu J, Profirovic J, Pan H, Vaiskunaite R, Voyno-Yasenetskaya T. G Protein betagamma subunits stimulate p114RhoGEF, a guanine nucleotide exchange factor for RhoA and Rac1: regulation of cell shape and reactive oxygen species production. *Circ Res.* 2003; 93:848–856. [PubMed: 14512443]
20. Matter K, Balda MS. Functional analysis of tight junctions. *Methods.* 2003; 30:228–234. [PubMed: 12798137]
21. Birkenfeld J, Nalbant P, Yoon SH, Bokoch GM. Cellular functions of GEF-H1, a microtubule-regulated Rho-GEF: is altered GEF-H1 activity a crucial determinant of disease pathogenesis? *Trends Cell Biol.* 2008; 18:210–219. [PubMed: 18394899]
22. Kakiashvili E, et al. GEF-H1 mediates tumor necrosis factor- α -induced Rho activation and myosin phosphorylation: role in the regulation of tubular paracellular permeability. *J Biol Chem.* 2009; 284:11454–11466. [PubMed: 19261619]
23. Zegers MM, O'Brien LE, Yu W, Datta A, Mostov KE. Epithelial polarity and tubulogenesis in vitro. *Trends Cell Biol.* 2003; 13:169–176. [PubMed: 12667754]
24. Yoshizaki H, et al. Activity of Rho-family GTPases during cell division as visualized with FRET-based probes. *J. Cell Biol.* 2003; 162:223–232. [PubMed: 12860967]
25. Sterpetti P, et al. Activation of the Lbc Rho exchange factor proto-oncogene by truncation of an extended C terminus that regulates transformation and targeting. *Mol Cell Biol.* 1999; 19:1334–1345. [PubMed: 9891067]
26. Krendel M, Zenke FT, Bokoch GM. Nucleotide exchange factor GEF-H1 mediates cross-talk between microtubules and the actin cytoskeleton. *Nat. Cell Biol.* 2002; 4:294–301. [PubMed: 11912491]
27. Cordenonsi M, et al. Cingulin contains globular and coiled-coil domains and interacts with ZO-1, ZO-2, ZO-3, and myosin. *J Cell Biol.* 1999; 147:1569–1582. [PubMed: 10613913]
28. Steed E, Balda MS, Matter K. Dynamics and functions of tight junctions. *Trends Cell Biol.* 2010; 20:142–149. [PubMed: 20061152]
29. Guillemot L, Citi S. Cingulin regulates claudin-2 expression and cell proliferation through the small GTPase RhoA. *Mol Biol Cell.* 2006; 17:3569–3577. [PubMed: 16723500]
30. Braga VM. Cell-cell adhesion and signalling. *Curr. Opin. Cell Biol.* 2002; 14:546–556. [PubMed: 12231348]
31. Noren NK, Arthur WT, Burridge K. Cadherin engagement inhibits RhoA via p190RhoGAP. *J. Biol. Chem.* 2003; 278:13615–13618. [PubMed: 12606561]
32. Abouhamed M, et al. Myosin IXa Regulates Epithelial Differentiation and Its Deficiency Results in Hydrocephalus. *Mol Biol Cell.* 2009

REFERENCES

33. Matter K, McDowell W, Schwartz RT, Hauri HP. Asynchronous transport to the cell surface of intestinal brush border hydrolases is not due to differential trimming of N-linked oligosaccharides. *J Biol Chem.* 1989; 264:13131–13139. [PubMed: 2526812]
34. Osler ME, Chang MS, Bader DM. Bves modulates epithelial integrity through an interaction at the tight junction. *J Cell Sci.* 2005; 118:4667–4678. [PubMed: 16188940]

35. Sourisseau T, et al. Regulation of PCNA and cyclin D1 expression and epithelial morphogenesis by the ZO-1-regulated transcription factor ZONAB/DbpA. *Mol Cell Biol.* 2006; 26:2387–2398. [PubMed: 16508013]
36. Jaffe AB, Kaji N, Durgan J, Hall A. Cdc42 controls spindle orientation to position the apical surface during epithelial morphogenesis. *J Cell Biol.* 2008; 183:625–633. [PubMed: 19001128]
37. Steed E, Rodrigues NT, Balda MS, Matter K. Identification of MarvelD3 as a tight junction-associated transmembrane protein of the occludin family. *BMC Cell Biol.* 2009; 10:95. [PubMed: 20028514]
38. Balda MS, et al. Functional dissociation of paracellular permeability and transepithelial electrical resistance and disruption of the apical-basolateral intramembrane diffusion barrier by expression of a mutant tight junction membrane protein. *J Cell Biol.* 1996; 134:1031–1049. [PubMed: 8769425]

**Figure 1.**

p114RhoGEF is a TJ associated RhoA GEF that regulates junction formation and the actin cytoskeleton. **(a)** Caco-2 and HCE cells transfected with non-targeting (Control) or siRNAs directed against p114RhoGEF (p114RG). Lysates were analysed by immunoblotting p114RhoGEF and α -tubulin. Uncropped images are shown figure S7. **(b - e)** HCE and Caco-2 cells were processed for immunofluorescence using antibodies against the proteins indicated. In **c**, cells were transfected with siRNAs targeting p114RhoGEF prior to immunofluorescence. Panels **b** and **c** are epifluorescence images whereas **d** and **e** are confocal xy and z line scans. **(f)** Levels of active Rho GTPases in HCE cells were measured after transfection of either control or p114RhoGEF targeting siRNAs. Shown are averages \pm 1SD, n=3. **(g,h)** Caco-2 and HCE cells were transfected with siRNAs (for p114RhoGEF, a pool containing siRNA1 and 2 were used) and then processed for immunofluorescence using antibodies against the indicated proteins **(g)** or fluorescent phalloidin to label f-actin **(h)**. For the columnar Caco-2 cells, two epifluorescence images are shown for the actin staining, one taken focusing on the apical region and one from the base of the cells. For the flat HCE cells, a single epifluorescence image is shown that includes lateral and basal actin staining. See figure S1 for other tight junction markers and experiments with individual siRNAs. Bars, 10 μ m.

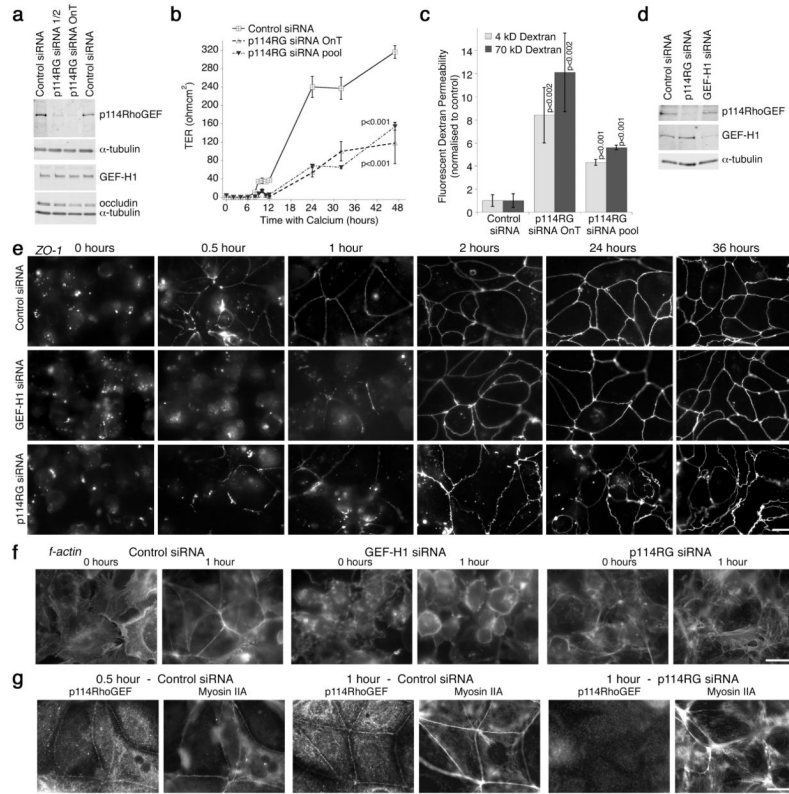
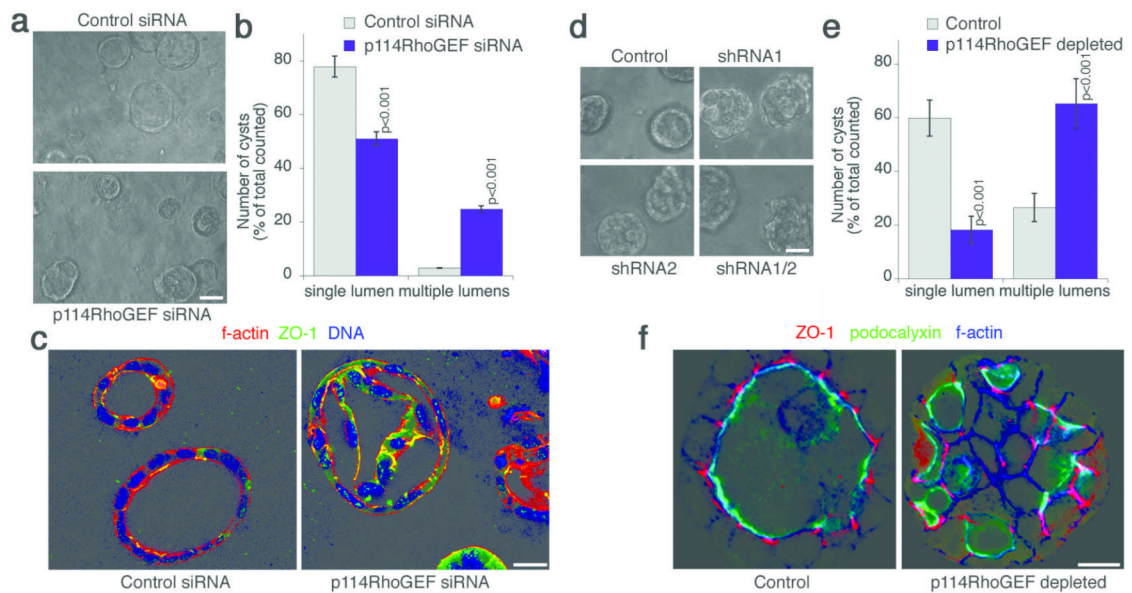
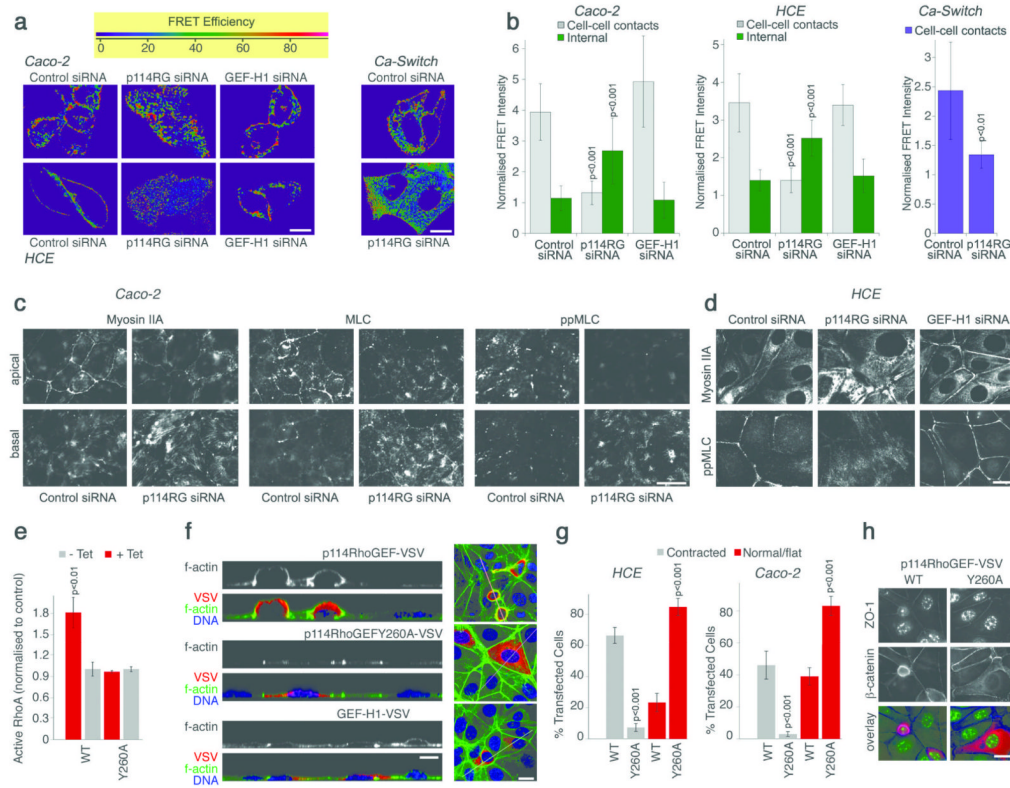


Figure 2. p114RhoGEF regulates epithelial barrier formation. (a-c) Caco-2 cells transfected with control or two different pools of p114RhoGEF specific siRNAs (OnT refers to the On-Target pool) were trypsinised and plated onto filters in low calcium media for 24 hours to prevent forming of cell-cell contacts. Expression of p114RhoGEF and other junctional proteins was assayed at the end of the experiment by immunoblotting (a). Uncropped images are shown figure S7. Normal calcium containing medium was added and cell contact formation was monitored during the next 48 hours by measuring transepithelial electrical resistance (b, shown are averages \pm 1SD, n=3). Paracellular tracer permeability was then determined using fluorescently labelled dextrans (c, shown are averages \pm 1SD, n=3). (d - h) Cells transfected with siRNAs and plated in low calcium followed by incubations in normal calcium were processed for immunoblotting (d, 24 hours of calcium, uncropped images are shown figure S7) or fixed at the indicated times and processed for immunofluorescence analysis using an epifluorescence microscope (e, ZO-1; f, f-actin; g, p114RhoGEF and myosin IIA). See figure S2 for additional junctional markers analysed. Focal planes for the epifluorescence images in panels f, g and h were chosen so that they include lateral and basal staining. Note, p114RhoGEF depleted cells, in contrast to GEF-H1 depleted, spread normally but did not assemble morphologically normal junctions. Bars, 10 μ m.

**Figure 3.**

p114RhoGEF regulates epithelial morphogenesis in three-dimensional cultures.

p114RhoGEF was depleted by transfecting siRNAs into Caco-2 cells (**a–c**) or by generating MDCK cells expressing shRNAs (**d–e**). The cells were then cultured in three-dimensional gels. After 5 days, the cultures were analysed by phase contrast microscopy (**a,d**) and quantified by counting cysts with a single lumen or structures with a disorganised appearance and multiple lumens (**b,e**; averages \pm 1SD; **b**, $n=3$; **e**, $n=5$). The cultures were then fixed and processed for analysis by confocal microscopy using the indicated antibodies and fluorescent labels (**c,f**). Bars, 30 μm (**a, d**) and 10 μm (**c, f**). See figure S2e for immunoblot analysis of p114RhoGEF expression.

**Figure 4.**

p114RhoGEF regulates RhoA signalling at cell junctions. **(a–b)** Cells were transfected with siRNAs and, after 2 days, with a RhoA FRET biosensor. RhoA activity was then imaged by gain of CFP fluorescence after acceptor bleaching. Shown are images of control, p114RhoGEF and GEF-H1 depleted cells taken from the apical part of the cells that contains the junctional complex **(a)**; see Fig. S3a for basal sections). Images to monitor Rho activity during junction formation were taken between 1 and 2 hours after adding calcium (Ca-Switch). Images were quantified by normalising FRET signals in specific regions (cell-cell contacts or interior cytoplasm) with the total FRET signal in the quantified fields **(b)**; averages \pm 1SD; n: Caco-2, 30 for control and p114RhoGEF and 12 for GEF-H1; HCE, 20 for control, 14 for p114RhoGEF, 12 for GEF-H1; Ca-Switch, 10). **(c–d)** Caco-2 cells **(c)** and HCE cells **(d)**, transfected with the specified siRNAs, were processed for immunofluorescence as indicated and analysed by epifluorescence microscopy. For Caco-2 cells, images taken from the apical and the basal regions are shown whereas a single image is shown for HCE cells that includes lateral and basal staining. **(e)** Levels of active RhoA were measured after tetracycline-induced expression of p114RhoGEF-VSV, labelled as WT, or p114RhoGEFY260A-VSV, labelled as Y260A, in MDCK cells. Shown are averages \pm 1SD, n=3. **(f)** HCE cells were transfected with the indicated constructs for p114RhoGEF and GEF-H1 expression and then processed for immunofluorescence and confocal microscopy. Shown are z line scans and xy sections. Note, the contracted appearance of cells expressing active p114RhoGEF. **(g)** Images from samples as those in panel f for HCE cells and analogous samples generated with Caco-2 cells (Fig. S5a) were quantified by counting transfected cells with a rounded/contracted appearance and cells that remained normal/flat. Shown are averages \pm 1SD, n=3. **(h)** HCE cells transfected as in panel f were stained for ZO-1 and β -catenin, and imaged by epifluorescence microscopy (the used antibody against ZO-1 crossreacts with a nuclear antigen in human cells). The overlay shows ZO-1 in green, β -catenin in blue and VSV in red. Bars, 10 μ m.

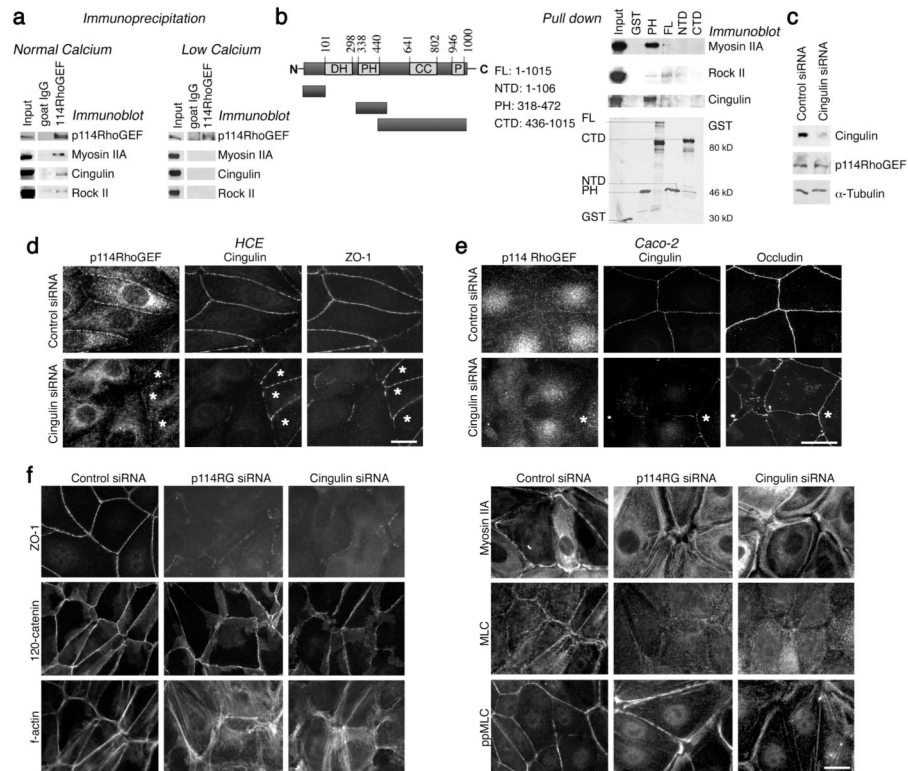


Figure 5. p114RhoGEF forms a complex with myosin II, cingulin and Rock II. **(a)** p114RhoGEF was immunoprecipitated from cell extracts of normally cultured Caco-2 cells or cells kept in low calcium to prevent junction formation. Beads conjugated with a non-related goat IgG were used as negative control. Coprecipitating proteins were analysed by immunoblotting as indicated. Uncropped images are shown figure S7. **(b)** GST fusion proteins containing different domains of p114RhoGEF were bound to beads and used for pull down experiments with Caco-2 cell extract. Pull downs were analysed by immunoblotting. **(c)** Cells were transfected with control or cingulin targeting siRNAs and expression of the indicated proteins was analysed by immunoblotting. **(d,e)** Caco-2 and HCE cells were transfected with siRNAs as in panel c and then fixed and processed for immunofluorescence to localise p114RhoGEF and junctional proteins. Shown are fields from depleted samples that still express some cingulin (labelled with asterisks). **(f)** HCE cells were transfected with siRNAs as indicated and then processed for immunofluorescence. All immunofluorescence images shown were acquired by epifluorescence microscopy and include lateral and basal structures. Bars, 10 μ m.